MOLECULAR AND CELLULAR BIOLOGY, July 2000, p. 4859–4869 Vol. 20, No. 13
0270-7306/00/$04.00+0

Arginine *N*-Methyltransferase 1 Is Required for Early Postimplantation Mouse Development, but Cells Deficient in the Enzyme Are Viable

MACIEJ R. PAWLAK, CHRISTINA A. SCHERER,† JIN CHEN,‡ MICHAEL J. ROSHON,§ AND H. EARL RULEY*

Department of Microbiology and Immunology, Nashville, Tennessee

Received 10 February 2000/Accepted 5 April 2000

Protein arginine *N*-methyltransferases have been implicated in a variety of processes, including cell proliferation, signal transduction, and protein trafficking. In this study, we have characterized essentially a null mutation induced by insertion of the U3βGeo gene trap retrovirus into the second intron of the mouse protein arginine *N*-methyltransferase 1 gene (*Prmt1*). cDNAs encoding two forms of Prmt1 were characterized, and the predicted protein sequences were found to be highly conserved among vertebrates. Expression of the *Prmt1*-β*geo* fusion gene was greatest along the midline of the neural plate and in the forming head fold from embryonic day 7.5 (E7.5) to E8.5 and in the developing central nervous system from E8.5 to E13.5. Homozygous mutant embryos failed to develop beyond E6.5, a phenotype consistent with a fundamental role in cellular metabolism. However, Prmt1 was not required for cell viability, as the protein was not detected in embryonic stem (ES) cell lines established from mutant blastocysts. Low levels of *Prmt1* transcripts (approximately 1% of the wild-type level) were detected as assessed by a quantitative reverse transcription-PCR assay. Total levels of arginine *N*-methyltransferase activity and asymmetric N^G,N^G-dimethylarginine were reduced by 85 and 54%, respectively, while levels of hypomethylated substrates were increased 15-fold. Prmt1 appears to be a major type I enzyme in ES cells, and in wild-type cells, most substrates of the enzyme appear to be maintained in a fully methylated state.

Methylation of arginine residues is one of many covalent modifications of eukaryotic proteins that occur concomitant with or shortly following translation. Two types of protein arginine methyltransferases have been classified according to their substrate specificity and reaction products (reviewed in reference 11). Type I enzymes catalyze the formation of N^G-monomethylarginine and asymmetric N^G,N^G-dimethylarginine, while type II enzymes catalyze the formation of N^G-monomethylarginine and symmetric N^G,N'^G-dimethylarginine. Most substrates for type I enzymes bind nucleic acid, usually RNA. These include heterogeneous nuclear RNA binding proteins (hnRNPs), which collectively contain 65% of the nuclear asymmetric dimethylarginine, as well as fibrillarin and nucleolin (19–21). The only known physiological substrate of symmetric (type II) arginine methyltransferase is myelin basic protein, a major protein component of the myelin sheath.

Genes encoding rat (*PRMT1*), human (*HRMT1L2*), and yeast (*RMT1*) type I enzymes have been characterized (12, 13, 17, 29). The mammalian genes appear to be ubiquitously expressed in all tissues (17, 29, 32). The yeast enzyme, which is not required for cell viability, accounts for over 85% of the protein dimethylarginine in the cell (12).

Type I enzymes have been implicated in a variety of processes, including cell growth control, signal transduction, and protein trafficking, but the biochemical and biological functions of arginine methylation have not been established. The enzymes preferentially methylate motifs rich in arginine and glycine (RGG boxes), a common feature of the RNA binding domains of hnRNPs (20). Arginine-methylated hnRNP A1 (24), but not Hrp1p (33), has lower affinity for RNA than the native protein, suggesting a potential mechanism for modulation of protein-RNA interactions. Levels of protein methylarginine may change in response to extracellular stimuli under circumstances in which biological responses are also suppressed by methyltransferase inhibitors. These include nerve growth factor-induced neurite outgrowth in PC12 cells (6) and mitogenic responses of lipopolysaccharide-treated B cells (16).

Interactions between the PRMT1 enzyme and potential signaling components have also emerged from yeast two-hybrid screens. The immediate-early gene product TIS21 (BTG2) and the leukemia-associated gene product BTG1 interact with PRMT1 and can modulate its enzymatic activity in vitro (17). TIS21 and BTG1 both belong to a family of mitogen-induced proteins implicated in negative regulation of the cell cycle. PRMT1 also binds to the cytoplasmic domain of the IFNAR1 chain of the alpha beta interferon receptor, while growth-inhibitory effects of interferon were suppressed by antisense oligonucleotides directed against the methyltransferase (1). Finally, a novel arginine methyltransferase (CARM1) associates with p160 coactivators and serves as a secondary coactivator of nuclear hormone receptors (4).

Other studies have identified a role for arginine methylation in protein trafficking. Shuttling of the yeast hnRNP-related proteins Np13p and Hrp1p between the nucleus and cytoplasm requires methylation by the Hmt1p methyltransferase (30). The human enzyme complements the shuttling defect, suggesting functional conservation between the two enzymes. Nuclear translocation of the large form of basic fibroblast growth factor may also depend on arginine methylation (23). In the presence of a methyltransferase inhibitor, basic fibroblast growth factor

* Corresponding author. Present address: Department of Microbiology and Immunology, Room AA4210 MCN, Vanderbilt University School of Medicine, 1161 21st Ave. South, Nashville, TN 37232-2363. Phone: (615) 343-1379. Fax: (615) 343-7392. E-mail: ruleye@ctrvax.vanderbilt.edu.

† Present address: Department of Microbiology, University of Washington, Seattle, WA 98195.

‡ Present address: Department of Medicine, Division of Rheumatology, Vanderbilt University School of Medicine, Nashville, TN 37232-2363.

§ Present address: Department of Emergency Medicine, Carolinas Medical Center, Charlotte, NC 28232-2861.

was not methylated and the protein did not localize to the nucleus.

The prevalence of N^G,N^G-dimethylarginine in RNA binding proteins and conservation among protein arginine *N*-methyltransferases underscore the potential biological importance of this posttranslational modification. However, a major issue arguing against a dynamic role for the type I enzymes in cell regulation concerns the possibility that arginine methylation is both constitutive and irreversible. While most substrates have not been characterized, some are known to exist only in a fully methylated state (18, 19). Moreover, no demethylase capable of removing dimethylarginine residues has been identified (11) and in the case of histones, turnover of dimethylarginine accompanies protein degradation (3).

Efforts to understand the biochemical function of mammalian arginine methyltransferases are complicated by several factors, including the existence of multiple enzymes and the fact that methyltransferase inhibitors nonspecifically target multiple processes in which *S*-adenosylmethionine serves as a methyl donor. In yeast, functional studies of arginine methylation have benefited greatly from genetic approaches that have led to the isolation of cells deficient in the enzyme. In principle, gene targeting strategies could be used for similar studies of the mammalian enzymes, assuming that the proteins are not required for cell viability.

The present study characterized a recessive early embryonically lethal mutation in a gene encoding the mouse ortholog of the human protein arginine *N*-methyltransferase 1 enzyme. The mutation was originally induced by gene entrapment in mouse embryonic stem (ES) cells and was selected during an in vitro screen for mutations in developmentally regulated genes (28). We now show that the enzyme is essential for early development, is a major source of arginine methyltransferase activity in ES cells, and yet is not required for cell viability. While proteins from mutant cells were significantly hypomethylated, most potential substrates in wild-type cells appeared to be blocked by prior methylation. The availability of Prmt1-deficient cells is expected to assist efforts to understand the function of this enzyme in normal cellular metabolism.

MATERIALS AND METHODS

Analysis of mutant and wild-type embryos. (i) Histology. Decidual swellings containing embryonic day 6.5 (E6.5) and E7.5 embryos were dissected in ice-cold phosphate-buffered saline (PBS), fixed in PBS containing 4% paraformaldehyde and 0.2% glutaraldehyde overnight at 4°C, dehydrated in a graded ethanol series, cleared in xylene, embedded in Paraplast X-tra (Polysciences), and sectioned. Serial sections (7 μm) were collected on slides, stained with hematoxylin and eosin (Sigma), and mounted in Permount (Fisher Scientific).

(ii) β-Galactosidase expression. E6.5 to E13.5 embryos were fixed in PBS containing fresh 2% paraformaldehyde and 2% glutaraldehyde for 30 min at 4°C, rinsed twice for 15 min each time and once for 1 h in ice-cold PBS, and stained overnight in PBS containing 0.02% NP-40, 0.01% sodium dodecyl sulfate (SDS), 2 mM $MgCl_2$, 5 mM $K_3Fe(CN)_6$, 5 mM $K_4Fe(CN)_6$, and 1 mg of 5-bromo-4-chloro-3-indolyl-β-D-galactopyranoside (X-Gal; Sigma), pH 7.2, per ml. Stained embryos were rinsed in PBS and visualized by dark-field microscopy.

Genotype analysis. Offspring bearing the *7.4.2* provirus were identified by Southern blot hybridization to a 1.3-kb *Stu*I fragment that contained genomic sequences of the *Prmt1* gene. E3.5 to E8.5 embryos were genotyped by PCR using a mixture of three primers, i.e., forward *7.4.2*#1 (5′ATATCCTTTTGTG AGACCCC), reverse *7.4.2*#2 (5′GGAAGGGCTCTGTCCTAA), and reverse *lacZ*#3 (5′CCTCTTCGCTATTACGCCAG). Each 25-μl PCR mixture contained 10 mM Tris-HCl (pH 8.3), 50 mM KCl, 1.5 mM $MgCl_2$, 200 μM each deoxyribonucleoside triphosphate, 1.25 U of Amplitaq (Perkin-Elmer Cetus), and each primer at 0.2 μM. Reactions proceeded through 40 cycles of denaturation (95°C for 1 min), primer annealing (55°C for 1 min), and primer extension (72°C for 2 min), followed by a final 10-min extension at 72°C. The resulting PCR products were resolved by 1.2% agarose gel electrophoresis and visualized by UV light after staining with ethidium bromide. DNAs from mice and embryos were isolated as described previously (35).

5′RACE. Transcribed cellular sequences present in *7.4.2*-βGeo fusion transcripts were cloned by rapid amplification of cDNA 5′ ends (5′RACE) using a 5′RACE kit (Gibco BRL) and following the manufacturer's instructions. First-strand cDNA was synthesized using 3 μg of total cellular RNA (5) and 0.2 μM reverse primer *lacZ*#3 (5′CCTCTTCGCTATTACGCCAG). After removal of the RNA template with RNase H (3.0 U), the cDNA was purified using BRL GlassMax spin cartridges and tailed with dCTP and terminal deoxynucleotidyltransferase. A 5-μl sample of tailed cDNA was amplified with 0.2 μM nested primer *lacZ*#2 (5′CTGCAAGGCGATTAAGTTGGG) and 0.2 μM Bethesda Research Laboratories anchor primer through 40 cycles of denaturation (95°C for 1 min) and primer annealing (55°C for 2 min) and extension (72°C for 3 min) and a 10-min extension at 72°C. The resulting PCR products were analyzed by Southern blot hybridization using a probe complementary to the first 20 nucleotides (nt) of the proviral long terminal repeat (LTR) (5′CCTACAGGTGGG GTCTTTCA). PCR products were gel purified (QIAquick gel extraction kit; QIAGEN), subcloned into the pCR plasmid vector (Invitrogen), and sequenced.

Isolation of *Prmt1* genomic and cDNA clones. The 189-nt *7.4.2* fusion transcript isolated via 5′RACE was used to screen an E8.5 mouse cDNA library (9). Two positive clones were identified out of a total of 10^6 plaques, and cDNA inserts of 1.1 kb and 600 nt were subcloned into the *Eco*RI site of pBluescript KS(−) (Stratagene) and sequenced. Subsequently, the 1.1-kb cDNA was used as a probe to rescreen the mouse E8.5 library and to screen an ES cell cDNA library (provided by B. Rosenberg, Massachusetts Institute of Technology). Altogether, 25 clones were isolated from the two libraries and sequenced.

Genomic DNA sequences flanking the provirus were cloned from a λFix II sv129 genomic library using the 189-nt 5′RACE product as a probe. Five clones contained a 1.3-kb *Stu*I fragment that hybridized to 5′RACE sequences immediately adjacent to the provirus. The 1.3-kb fragment was subcloned into the *Eco*RV site of pBluescript KS(−) (Stratagene) and sequenced.

Northern blotting and RT-PCR. Total cellular RNA was isolated from various C57BL/6J mouse tissues (liver, heart, lung, kidney, ovary, brain, and spleen), whole wild-type embryos, and ES cells of the D3 line via the method of Chomczynski and Sacchi (5). A 15-μg sample of each RNA was denatured with formamide, electrophoretically separated on 1% formaldehyde agarose gels, transferred to a HyBond-N+ filter (Amersham), and hybridized to [α-^{32}P]dCTP-labeled probes (10).

Reverse transcription (RT)-PCR was performed as previously described (15). Briefly, 20 μg of total cellular RNA was treated with RNase-free DNase (5 U; Gibco BRL), extracted with phenol-chloroform, precipitated in ethanol, and resuspended in 20 μl of H_2O. A 5-μl portion of each RNA sample was reverse transcribed using a reverse oligonucleotide primer (5′CAGCAAACATGCAGA GGATGCCAGT to detect the 54-nt *Prmt1* alternative exon or 5′GTGCACGC GCTGGTGGCTTACTTCAA to quantify *Prmt1* transcripts in wild-type and mutant cells), 200 U of SuperScript II (Gibco BRL), and 500 μM each deoxyribonucleoside triphosphate. After treatment with 3.0 U of RNase H (Gibco BRL), sequences corresponding to the *Prmt1* 54-nt alternative exon were amplified using 2 μl of the first-strand cDNA, 0.2 μM forward primer (5′GCGAA CTGCATCATGGAG), and 0.2 μM reverse primer (5′ACATCCAGCACCAC CTTG) as described above. For quantitative analysis of *Prmt1* transcripts, the PCRs used 5′GACAGCCATTGAGGACCGAC and 5′CCAATGCCTGCCTC ATAA as forward and reverse primers, respectively.

Mapping. An interspecific backcross [(C57BL/6J × *Mus spretus*)F_1 × *M. spretus*] DNA panel from the Jackson Laboratory community resource (26) was used to map the *Prmt1* locus. Genomic DNAs from C57BL/6J and *M. spretus* were digested with various restriction enzymes and blot hybridized to the 1.3-kb *Prmt1* genomic probe to detect restriction fragment length polymorphism (RFLP) between the two strains. Filters containing *Msp*I-digested genomic DNAs from the 94 backcrosses and two parental strains (BSS panel) were obtained from the Jackson Laboratory and hybridized to the 1.3-kb *Prmt1* genomic probe. Each DNA was scored for the presence of the C57BL/6J allele, and the results were analyzed against the Jackson Laboratory database to determine the position on the existing map.

DNA sequencing. DNA sequencing reactions used the BigDye Terminator Cycle Sequencing Kit (ABI) and were analyzed on a Prism 377 DNA Sequencer. Templates were either subcloned into pBluescript (Stratagene) or sequenced directly from phage DNAs. Primers were either T3 and T7 or oligonucleotide primers corresponding to various regions of *Prmt1*. DNA sequences were compiled with Sequencher 3.0 software (Gene Codes Corporation), and sequence homology searches were performed using the BLAST algorithm (2).

Isolation of ES cells. ES cells lines were isolated from E3.5 blastocysts as described previously (35) and were maintained on 0.1% gelatinized tissue culture plates in ES cell medium (high-glucose Dulbecco modified Eagle medium [Gibco] supplemented with 15% preselected fetal bovine serum [Hyclone; heat inactivated at 55°C for 30 min], 0.1 mM 2-mercaptoethanol, and 100 mM nonessential amino acids [Gibco]) supplemented with 1,000 U of leukemia inhibitory factor (ESGRO; Gibco) per ml. Cultures were trypsinized every 2 days and replated at a 1:3 ratio with either a feeder layer of gamma-irradiated mouse embryo fibroblasts for maintenance of the cell line or for at least 3 generations without feeder layers for isolation of DNA, RNA, and cell extracts.

Western blotting analysis. Samples (200 μg of protein each) were mixed with an equal volume of 2× Laemmli loading buffer (27), boiled for 5 min, and fractionated by SDS–10% polyacrylamide gel electrophoresis. Proteins were transferred onto PolyScreen polyvinylidene difluoride membrane (NEN Life Sciences) in Tris-glycine buffer (27). Polyclonal serum from rabbits immunized against recombinant rat PRMT1 (32) was diluted 1:3,000 in TBST (10 mM

Tris-HCl [pH 8.0], 150 mM NaCl, 0.05% Tween 20) containing 5% milk and bound to proteins for 1 h. Membranes were washed three times for 10 min each time in TBST, incubated with a 1:10,000 dilution of peroxidase-conjugated anti-rabbit secondary antibody (Santa Cruz Biotechnology, Inc.) in TBST for 30 min, and detected by enhanced chemiluminescence assay (Amersham).

Methyltransferase assays. For protein extraction, cells were harvested at 75% confluency, washed twice, scraped into ice-cold PBS, pelleted, and resuspended in 1 ml (per 10-cm-diameter plate) of ice-cold reaction buffer (50 mM Tris-HCl [pH 7.6], 0.1 mM EDTA, 0.1 mM dithiothreitol, 1 mM phenylmethylsulfonyl fluoride). The cell suspensions were sonicated on ice with two 15-s bursts using a microtip sonicator (XL2015; Heat Systems) at a setting of 4.0 and clarified by centrifugation at 10,000 × *g* for 30 min, and the supernatant was flash frozen in an ethanol–dry-ice bath. Protein concentrations were determined by a modified Lowry assay (DC Protein Assay; Bio-Rad).

Reactions to measure methyltransferase activity were performed in reaction buffer supplemented with 50 μM *S*-adenosyl-L-[*methyl*-^{3}H]methionine (Amersham; adjusted to 5,000 dpm/pmol with unlabeled AdoMet), 100 μM R3 peptide (21), and either wild-type or mutant cell extract. Reactions to measure the methylation status of proteins in cell extracts were performed in reaction buffer containing 50 μM *S*-adenosyl-L-[*methyl*-^{3}H]methionine and either equal amounts of wild-type and mutant cell extracts or wild-type cell extract alone. Methylation reaction mixtures contained 140 μg of total protein in 140 μl and were incubated at 36°C. Aliquots (20 μl) were withdrawn at different intervals, added to 20 μl of 2× SDS sample buffer, and heated to 100°C for 5 min to stop the reaction. The samples were diluted into 1 ml of PBS, and the incorporated *methyl*-^{3}H was determined via a filter binding assay (20).

Amino acid analysis. Analysis of methylated arginine derivatives in total cell lysates was performed by the Vanderbilt-Ingram Cancer Center Peptide Sequencing and Amino Acid Analysis Shared Resource. Briefly, samples were hydrolyzed with 6N HCl (110°C for 18 h) in vacuo in a Waters PicoTag apparatus, derivatized by the Waters AccQ Tag amino acid analysis method, and separated on a Waters AccQ Tag C_{18} column (3.8 by 150 mm) developed with a 1:40 dilution of eluent A (Waters). Methylated arginine standards (N^G-monomethylarginine, asymmetric N^G,N^G-dimethylarginine, and symmetric N^G,N'^G-dimethylarginine; Sigma) were analyzed under the same conditions, and their elution profiles were compared to the elution profiles of cell protein hydrolysates.

Nucleotide sequence accession numbers. The genomic sequences reported here have been submitted to GenBank and assigned accession no. AF232718 (see Fig. 4B), AF232716, and AF232717 (see Fig. 5).

RESULTS

Expression of the gene disrupted by the *7.4.2* provirus. The *7.4.2* mutation was induced by the U3βGeoSupF retrovirus in mouse ES cells and identified during an in vitro screen for inserts into developmentally regulated genes. The provirus expresses a β-galactosidase–neomycin phosphotransferase fusion protein encoded by transcripts that initiate in the flanking cellular DNA. The *7.4.2* mutation was chosen for germ line transmission because expression of the β-galactosidase fusion gene was induced during differentiation in vitro (28). Undifferentiated *7.4.2* ES cells stained mostly white but showed an increase in *lacZ* expression following differentiation into embryoid bodies. *lacZ* expression was also developmentally regulated in vivo (Fig. 1). β-Galactosidase activity was not detected in blastocyst stage embryos (E3.5) but was induced in postimplantation embryos as early as E6.5. At E6.5, diffuse staining was evident throughout the whole embryonic portion of the egg cylinder, and by E7.5, staining appeared strongest along the midline of the neural plate and in the forming head fold (Fig. 1A). Diffuse staining was also visible throughout the rest of the neural plate and in the primitive streak. E8.5 embryos stained mostly in the areas corresponding to the developing central nervous system, including both the brain and spinal cord regions. Intense staining was visible in the anteriormost aspect of the developing brain (prosencephalon) and continued caudally through the mesencephalon, rhombencephalon, and fusing neural folds (Fig. 1B to D). Neural-tube staining was restricted to the lateral sides, and the floor plate did not stain at all. Staining was also apparent in the primitive streak, brachial arches, notochord, and heart anlage. Again, diffuse staining was visible throughout the embryos. Between E9.5 and E13.5, this diffuse staining pattern became even more apparent; however, darker staining was still visible in the telencephalon, neural tube, heart, and first and second brachial arches (Fig. 1E). In addition, staining could be seen in the developing forelimb bud. At all of the developmental stages examined, X-Gal staining was widespread in the embryo but absent from extraembryonic tissues, including the yolk sac, extraembryonic ectoderm, and ectoplacental cone.

Mice homozygous for the *7.4.2* mutation die in utero. Initial characterization of 48 offspring from intercrosses between *7.4.2* heterozygotes revealed that none of the viable offspring were homozygous for the provirus. Out of 48 offspring genotyped, 34 heterozygotes and 14 wild-type pups were recovered, a ratio of approximately 2.5:1. This situation strongly suggested that the *7.4.2* provirus disrupted a gene essential for murine development and that homozygous embryos die in utero. As *7.4.2* mice have been maintained for over 10 generations, the embryonically lethal phenotype appears to be tightly linked to the provirus.

In order to determine the time of embryonic death, 187 embryos obtained by crossing *7.4.2* heterozygotes were dissected from the uterine decidua between E6.5 and E10.5 and genotyped by PCR (Fig. 2B). Since the sequences flanking the provirus were cloned (see below), wild-type and mutant alleles could be easily distinguished based on the size of the PCR product (Fig. 2A). No homozygous embryos were recovered at E10.5 and E8.5, although a large number of empty resorption sites were observed (between 16 and 30% of the litter). Heterozygous embryos were morphologically indistinguishable from their wild-type littermates. The ratio of wild-type to heterozygous embryos indicated that *7.4.2* homozygotes die before E8.5, accounting for the large proportion of resorption sites. Only one homozygous embryo was recovered at E7.5. This embryo was much smaller than its wild-type and heterozygous littermates and resembled a severely disorganized and degenerated egg cylinder. Two homozygous embryos recovered at E6.5 also displayed an obvious developmental delay in embryonic portions of the embryo, while extraembryonic tissues seemed to develop normally. Other small and partially resorbed embryos dissected at the E6.5 and E7.5 stages were genotyped as heterozygotes. However, this probably reflects contamination of homozygous mutant embryos with maternal tissue, accounting for the lower-than-expected yield of *7.4.2* homozygotes at this stage. Since we were able to recover morphologically normal homozygous mutant blastocysts (E3.5), which were present at the expected ratio, it is likely that embryonic death occurs shortly after implantation (E4.5) but before the onset of gastrulation (E6.5).

To better document mutant phenotypes, histologic sections were prepared from embryos present in uterine decidual swellings at E6.5 to E7.5 (Fig. 3; Table 1). Similar studies of embryos from wild-type litters served to establish the nature and frequency of nonspecific abnormalities unrelated to the *7.4.2* mutation. At E6.5, 28% of the sectioned embryos derived from heterozygous crosses displayed severe defects, a number much higher than that observed in litters from wild-type crosses (about 5%). Morphological abnormalities observed among the majority of aberrant embryos were consistent and different from the ones observed in the control litters. The presumptive *7.4.2* homozygotes were generally retarded in growth, especially in embryonic portions of the conceptus, and displayed signs indicating that they were undergoing resorption. Egg cylinders of these mutants were severely attenuated and often fragmented and lacked an organized two-layered cellular structure. No proamniotic cavities, ectoplacental cavities, or amniotic folds were observed in aberrant embryos. However, the mutant embryos appeared to develop normal ectoplacental

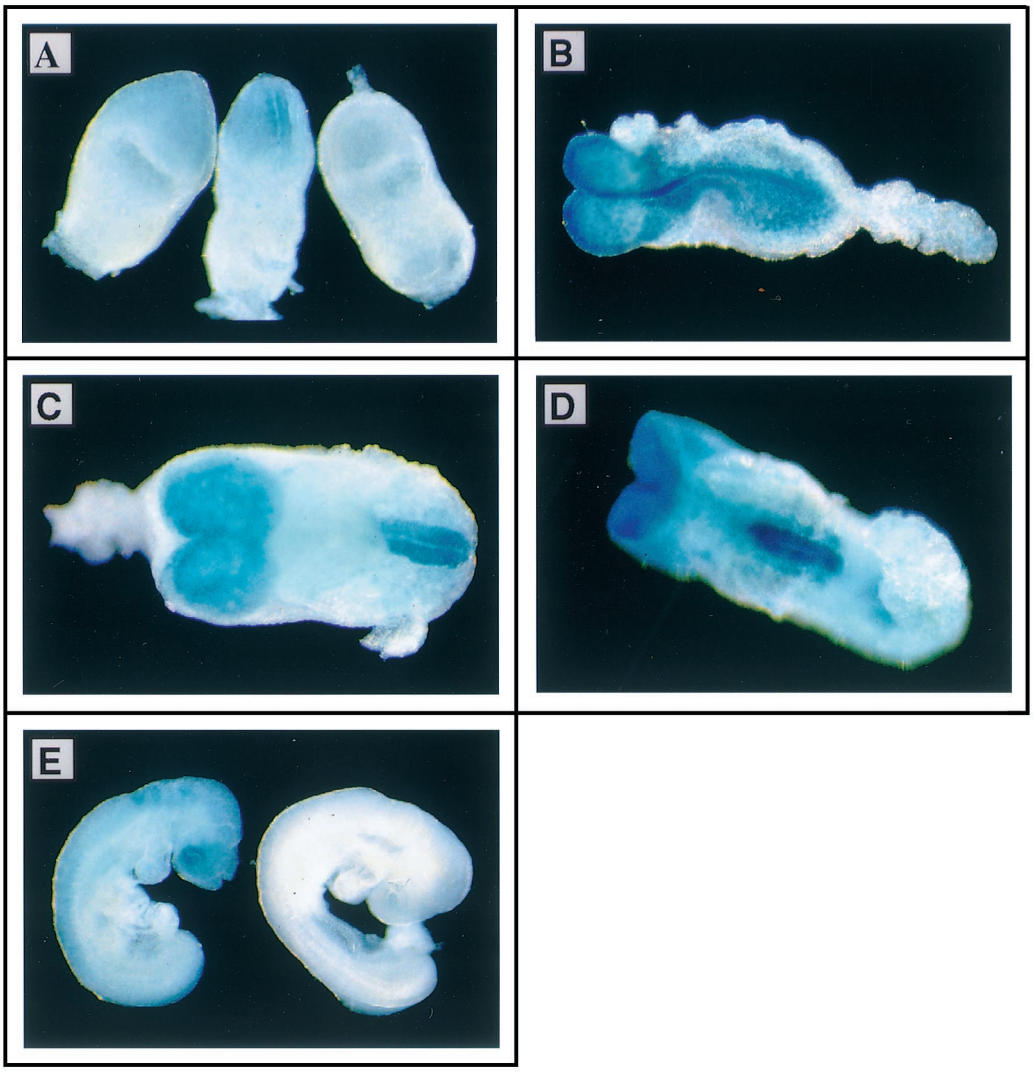

FIG. 1. Embryonic expression of the *7.4.2*-βGeo fusion gene. Spatial and temporal expression of the *Prmt1* gene was assessed by staining *Prmt1*$^{+/-}$ embryos with X-Gal. (A) Left and middle, E7.5 heterozygous embryos showing strong *lacZ* expression along the midline of the neural plate. X-Gal staining is not detected in the extraembryonic ectoderm. Right, E7.5 wild-type embryo. (B to D) Dorsal (B), rostral (C), and ventral (D) views of E8.5 heterozygous embryos showing *lacZ* expression in the developing brain and fusing neural folds. Expression extends from the prosencephalon through the mesencephalon and rhombencephalon to the posteriormost aspect of the neural folds. *lacZ* expression is not detected in floorplate cells. (E) Left, lateral view of an E9.5 heterozygous embryo showing *lacZ* expression in the developing brain, eye, and closed neural tube; diffuse staining is visible throughout the whole embryo. Right, lateral view of E9.5 wild-type embryo.

cones and extraembryonic membranes and appeared to make good contact with the uterus. At E7.5, 23% of the decidui contained aberrant embryos (versus 5% in control litters). While the majority of the resorption sites were empty, some contained remnants of retarded and disintegrated egg cylinders. In summary, it appears that *7.4.2* homozygotes implant into the uterus but fail to develop beyond the early egg cylinder stage. Embryonic lethality of these mutants occurs shortly after implantation, and resorption is initiated prior to gastrulation.

Characterization of the gene disrupted by the *7.4.2* provirus. Transcribed cellular sequences appended to proviral βGeo sequences were cloned by 5′RACE. This exploits the fact that cell-virus fusion transcripts initiate in the flanking cellular DNA and terminate at the poly(A) site in the 5′ LTR. The resulting 189-nt 5′RACE product was sequenced (Fig. 4A) and used to probe Northern blots of cellular RNA from 7.4.2 cells. A single 1.3-kb transcript was detected (data not shown). The 5′ RACE fragment was subsequently used to isolate cDNAs of the mutated gene and genomic DNA sequences surrounding the *7.4.2* provirus.

The 5′ end of the consensus cDNA sequence (see below) matched regions of the 5′RACE product and also included a small region located in the genomic DNA sequence near the site of virus integration (Fig. 4). The first 110 nt of the 5′RACE product (shown as open and shaded boxes in Fig. 4A) and a 54-nt region of the flanking genomic sequence (shown as a shaded box in Fig. 4B) were both contained in the cDNA sequence. The 54-nt genomic sequence is flanked by consensus splice site sequences, further suggesting that it is an exon. The 5′RACE product contains this exon (shaded box), as well as a 56-nt sequence (open box, Fig. 4A) that is presumably derived from one or more upstream exons. The last 79 nt of the 5′RACE product (extending to the provirus integration site) match the genomic DNA sequence immediately upstream of the provirus and represent transcribed intron sequences that extend into the provirus.

A

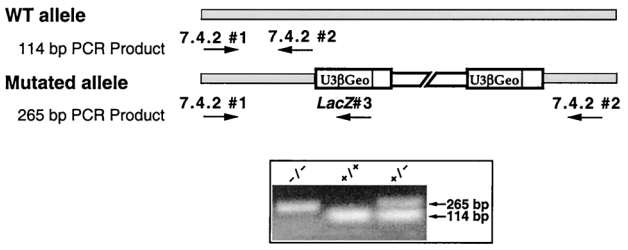

B

Age (E)	Total No.	Embryos +/+	Embryos +/-	Embryos -/-	Resorbed
10.5	57	20	28	0	9
8.5	37	7	18	0	12
7.5	61	18	39	1	3
6.5	32	7	21	2	2
3.5	13	2	7	4	0

FIG. 2. Timing of embryonic death. Strategy for PCR-based genotyping (A). PCRs used a combination of three primers complementary to cellular (primers 1 and 2) and viral (primer 3) DNA sequences, as shown in schematic representations of the normal and disrupted alleles. Normal and mutant alleles generated PCR products of 114 (primers 1 and 2) and 265 (primers 1 and 3) nt, respectively. The PCR products were visualized following agarose gel electrophoresis and staining with ethidium bromide (box). Primers 1 and 2 did not amplify sequences from the mutant allele, presumably because of the size (10.3 kb) of the intervening U3βGeo provirus. WT, wild type. (B) Genotypes of E3.5 blastocysts and E6.5 to E10.5 embryos. Mice heterozygous for the *7.4.2* provirus were mated, and the resulting embryos were genotyped at various times postcoitus.

TABLE 1. Embryonically lethal phenotype caused by the *Prmt1* mutation[a]

Cross	Embryo age (days)	Total no. of embryos	No. abnormal	No. resorbed	% Failure
Ht × Ht	6.5	29	6	2	27.6
Ht × Ht	7.5	31	3	4	22.6
WT × WT	6.5	23	1	0	4.4
WT × WT	7.5	20	1	0	5.0

[a] Mice heterozygous for the *Prmt1* mutation (Ht) were mated, and embryos were examined at E6.5 and E7.5. Embryos were classified based on their appearance as normal, abnormal, or resorbed. The percentage of embryos that failed to develop normally as assessed by abnormal appearance and resorption was as expected for a recessive lethal mutation. WT, wild type.

The 1.3-kb genomic DNA fragment hybridized to a single 1.3-kb *Stu*I fragment in DNA from wild-type mice (Fig. 4C). An additional 10.5-kb fragment was detected in DNA of mice heterozygous for the *7.4.2* provirus. A fragment of the same size also hybridized to a virus-specific probe, consistent with insertion of an intact βGeo provirus (Fig. 4C). In addition, no rearrangements were observed in either the virus or flanking cellular DNA.

The composite cDNA sequence of the gene disrupted by the *7.4.2* provirus is depicted in Fig. 5. Open reading frames of 353 or 371 amino acids are present, depending on the absence or presence of the 54-nt exon. Although the first ATG in the composite cDNA sequence is in a favorable context for translation initiation, there is no in-frame upstream stop codon. Comparison of the composite cDNA sequence to 112 murine and 209 human expressed sequence tags obtained from the National Center for Biotechnology Information dbEST data-

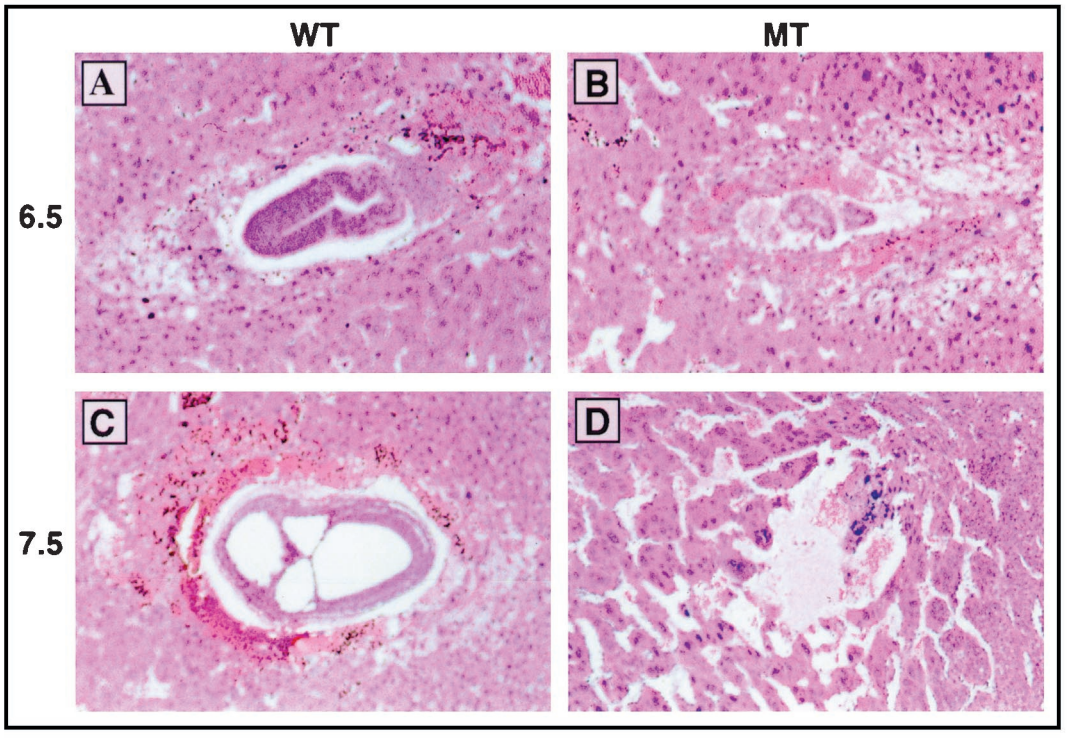

FIG. 3. Phenotype of *Prmt1*$^{-/-}$ embryos at E6.5 to E7.5. Mice heterozygous for the *7.4.2* provirus were mated, and embryos were examined at various stages of embryonic development. Sections through wild-type (WT) (A and C) and mutant (MT) (B and D) embryos at E6.5 (A and B) and E7.5 (C and D) were stained with hematoxylin and eosin.

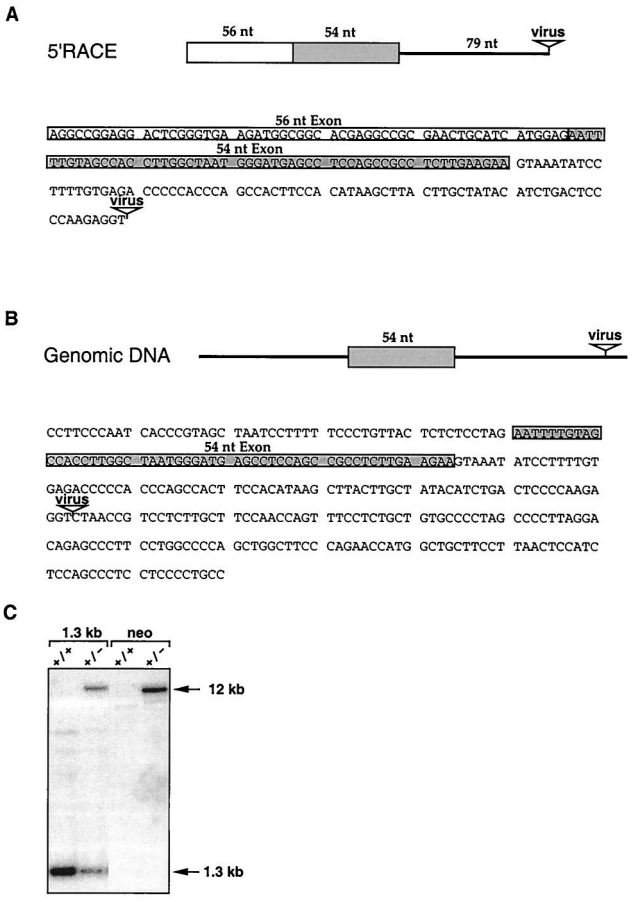

FIG. 4. The *7.4.2* provirus inserts into an intron of the protein arginine *N*-methyltransferase gene. (A) Fusion transcripts extending into the U3βGeo provirus were isolated by 5′RACE and sequenced. Sequences of 56 and 54 nt (boxed) are from separate exons, while the 79-nt region immediately 5′ of the provirus integration site is intron derived. (B) Genomic sequences containing the site of provirus integration were cloned as a 1.3-kb *Stu*I fragment and partially sequenced. The 54-nt alternatively spliced exon (boxed) is located 79 nt 5′ of the provirus. (C) Southern blot analysis of wild-type (+/+) and heterozygous (+/−) mouse cells. *Stu*I-cleaved cellular DNAs were probed with the *Stu*I fragment that contains the site of provirus integration (lanes 1 and 2) or with a *neo*-specific probe (lanes 3 and 4). Since *Stu*I does not cleave U3βGeo, the provirus-occupied allele (12 kb) is shifted by the size of the provirus.

base revealed none that extended beyond the 5′ end of the composite cDNA (data not shown). The 54-nt exon was present in 5 out of 13 cDNAs from the E8.5 library but only in 1 of 10 cDNAs from the ES cell library.

The *7.4.2* gene encodes a protein arginine *N*-methyltransferase. A BLAST search of the nucleic acid databases with the composite *7.4.2* cDNA sequence returned matches with rat (PRMT1), human (HRMT1L2), and yeast (RMT1/HMT1) protein arginine *N*-methyltransferases. The rat cDNA lacked the 54-nt sequence corresponding to the presumed alternative exon (17). However, this sequence was present in two out of three variants of the human gene (29). The mouse and rat sequences are identical at the protein level, except for the 18-amino-acid segment missing from the rat protein that corresponds to the 54-nt alternative exon. The mouse and human proteins are 95% identical, differing at only two internal positions (E118 to V and H179 to Y) and 10 amino-terminal residues present in the mouse (and rat) protein but absent from human HRMT1L2 (Fig. 5). The mouse protein also shares 45% overall identity with the *Saccharomyces cerevisiae* RMT1 enzyme (12) and 11% identity with the *Escherichia coli* L11 methyltransferase (34). This high degree of phylogenetic conservation was especially evident in regions containing consensus methyltransferase motifs (Fig. 5). Based on these sequence comparisons, we concluded that the gene disrupted by the *7.4.2* provirus is the murine ortholog of the rat and human protein arginine *N*-methyltransferases (PRMT1 and HRMT1L2, respectively). The *7.4.2* gene was provisionally named *Prmt1* for mouse arginine *N*-methyltransferase 1.

***Prmt1* is widely expressed in mouse tissues and in embryos.** The pattern of β-galactosidase expression suggested that *Prmt1* is regulated in a tissue- and/or stage-specific manner. Analysis of total cellular RNAs from several mouse tissues (liver, heart, lung, kidney, ovary, brain, and spleen); E8.5, E9.5, and E11.5 mouse embryos; and the D3 ES cell line by Northern blot hybridization revealed that *Prmt1* encodes a 1.3-kb transcript present in all of the RNAs examined (Fig. 6A). In general, the transcript seems to be more abundant in ES cells and embryos than in adult tissues. *Prmt1* transcript levels also varied among all of the adult tissues tested, with the highest expression in the ovaries and uterus and the lowest in the liver. Of the three brain regions examined, only the cerebellum displayed a slightly higher transcript level.

In order to determine the expression pattern of the transcripts containing the 54-nt alternatively spliced exon, RT-PCR analysis was performed using the RNAs described above and primers flanking this exon. RT-PCR revealed that transcripts containing the message encoded by the 54-nt exon were uniformly present in ES cells, embryos, and all of the adult tissues tested (Fig. 6B).

***Prmt1* maps to mouse chromosome 7.** The chromosomal location of the mouse *Prmt1* locus was determined by inter-

```
                M  A  A  A  E  A  A  N  C  I  M  E  N  F  V          15
GGACTCGGGTGAAGATGGCGGCAGCCGAGGCCGCGAACTGCATCATGGAGAATTTTGTAG        60
A  T  L  A  N  G  M  S  L  Q  P  P  L  E  E  V  S  C  G  Q          35
CCACCTTGGCTAATGGGATGAGCCTCCAGCCGCCTCTTGAAGAAGTTTCCTGTGGCCAAG       120
A  E  S  S  E  K  P  N  A  E  D  M  T  S  K  D  Y  Y  F  D          55
CAGAAAGTAGTGAGAAGCCCAACGCTGAGGACATGACATCCAAAGACTACTACTTTGACT       180
S  Y  A  H  F  G  I  H  E  E  M  L  K  D  E  V  R  T  L  T          75
CCTATGCCCACTTTGGCATCCACGAGGAGATGCTGAAGGATGAGGTGCGCACCCTCACAT       240
Y  R  N  S  M  F  H  N  R  H  L  F  K  D  K  V  V  L  D  V          95
ACCGCAACTCCATGTTTCACAATCGGCATCTCTTCAAAGACAAGGTGGTGCTGGATGTGG       300
G  S  G  T  G  I  L  C  M  F  A  A  K  A  G  A  R  K  V  I         115
GCTCAGGCACTGGCATCCTCTGCATGTTTGCTGCCAAGGCGGGGGCCCGCAAGGTTATTG       360
G  I  E  C  S  S  I  S  D  Y  A  V  K  I  V  K  A  N  K  L         135
GGATTGAGTGTTCCAGTATCTCCGATTATGCTGTGAAGATTGTCAAAGCCAACAAGTTAG       420
D  H  V  V  T  I  I  K  G  K  V  E  E  V  E  L  P  V  E  K         155
ACCATGTGGTGACCATCATCAAGGGCAAGGTGGAGGAGGTGGAGCTGCCCGTGGAGAAGG       480
V  D  I  I  I  S  E  W  M  G  Y  C  L  F  Y  E  S  M  L  N         175
TGGACATCATCATCAGCGAGTGGATGGGTTACTGCCTCTTCTACGAGTCCATGCTCAACA       540
T  V  L  H  A  R  D  K  W  L  A  P  D  G  L  I  F  P  D  R         195
CCGTGCTGCACGCTCGGGACAAGTGGCTGGCACCCGATGGCCTCATCTTCCCAGACCGGG       600
A  T  L  Y  V  T  A  I  E  D  R  Q  Y  K  D  Y  K  I  H  W         215
CCACCTTGTATGTGACAGCCATTGAGGACCGACAATATAAAGACTACAAGATCCACTGGT       660
W  E  N  V  Y  G  F  D  M  S  C  I  K  D  V  A  I  K  E  P         235
GGGAGAACGTGTATGGCTTTGATATGTCCTGCATTAAAGACGTGGCCATCAAGGAGCCCC       720
L  V  D  V  V  D  P  K  Q  L  V  T  N  A  C  L  I  K  E  V         255
TGGTGGACGTGGTGGACCCAAAGCAGCTGGTCACCAATGCCTGCCTCATAAAGGAGGTGG       780
D  I  Y  T  V  K  V  E  D  L  T  F  T  S  P  F  C  L  Q  V         275
ACATTTACACAGTCAAGGTGGAGGACCTGACCTTCACCTCCCCCTTCTGCCTGCAAGTGA       840
K  R  N  D  Y  V  H  A  L  V  A  Y  F  N  I  E  F  T  R  C         295
AGAGGAACGACTACGTGCACGCGCTGGTGGCTTACTTCAACATCGAGTTCACCCGATGCC       900
H  K  R  T  G  F  S  T  S  P  E  S  P  Y  T  H  W  K  Q  T         315
ACAAGAGGACCGGCTTCTCCACCAGTCCTGAGTCCCCGTACACACACTGGAAGCAGACTG       960
V  F  Y  M  E  D  Y  L  T  V  K  T  G  E  E  I  F  G  T  I         335
TGTTCTACATGGAGGACTACCTAACAGTGAAGACTGGCGAGGAGATCTTTGGCACCATTG      1020
G  M  R  P  N  A  K  N  N  R  D  L  D  F  T  I  D  L  D  F         355
GAATGAGGCCCAATGCCAAAAACAATCGTGACTTGGACTTTACCATCGACCTGGACTTCA      1080
K  G  Q  L  C  E  L  S  C  S  T  D  Y  R  M  R  *                 371
AGGGTCAGCTGTGTGAGCTCTCTTGTTCCACCGACTACCGGATGCGCTGAGGAGGTGCCA      1140
GGCTGGCCCTCCTGCAGAAGGGGGCTCGGGGGGATGGGCTTGGGGGATGGGGGGGTACAT      1200
CGTGACTGTGTTTTTCATAACTTATGTTTTTATATGGTTGCGTTTATGCCAATAAATCCT      1260
CAGCTGACCATGAAAAAAAAAA                                            1282
```

FIG. 5. Nucleotide and deduced amino acid sequences of the murine *Prmt1* gene. The 1,282-nt cDNA sequence, including additional sequences obtained by 5′RACE, is shown. The predicted amino acid sequence of the Prmt1 protein is presented above the cDNA sequence. Sequences corresponding to an alternatively spliced 54-nt exon and poly(A) site are underlined. The same exon is located just 5′ of the provirus integration site (Fig. 4B). Conserved arginine *N*-methyltransferase motifs I, post-I, II, and III are shaded. Differences between the mouse and human proteins are in boldface type.

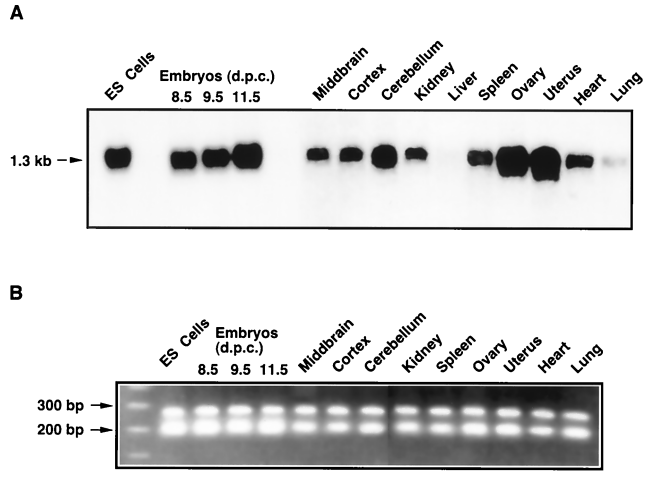

FIG. 6. Distribution of *Prmt1* transcripts in embryos and tissues. (A) Northern blot hybridization of RNAs from various mouse tissues, embryos, and the D3 ES cell line (as indicated) to a ^{32}P-labeled 1.1-kb *Prmt1* cDNA probe. The position of the *Prmt1*-encoded 1.3-kb transcript is indicated at the left. The autoradiogram was exposed for 24 h. (B) RT-PCR analysis of the alternatively spliced 54-nt exon. *Prmt1* transcripts were reverse transcribed from various RNAs (see above) using an oligonucleotide primer complementary to the *Prmt1* sequence 3′ of the 54-nt exon and amplified by using primers that flank that exon. RT-PCR products of 266 and 212 bp are expected for transcripts with and without the 54-nt exon, respectively. d.p.c., days postconception.

specific backcross analysis using the Jackson Laboratory interspecific backcross panel (C57BL/6JEi × SPRET/Ei)F_1 × SPRET/Ei. This mapping panel has been initially typed for over 450 chromosomal and X-linked loci spread among the autosomes, as well as the X chromosome, and the resulting genetic map was anchored to published maps by mapping known loci, simple sequence length polymorphisms, and loci defined by endogenous retroviruses. In order to identify a suitable RFLP for use in mapping studies, C57BL/6JEi and *M. spretus* genomic DNAs were digested with a panel of restriction enzymes and analyzed by Southern blot hybridization using the 1.3-kb *Prmt1* probe. Subsequently, an *Msp*I RFLP was used to map the *Prmt1* locus on mouse chromosome 7 between Fig1 and D7Bwg0826e (Fig. 7). No known mutation or disease phenotype is linked to the *Prmt1* locus.

Isolation of ES cells from mutant blastocysts. In principle, the *Prmt1* mutation could be a cell-lethal defect in which mutant embryos persist beyond implantation due to maternal stores of mRNA, enzyme, or methylated substrates. Although most maternal RNA is rapidly degraded following the first cell division, the Prmt1 enzyme or methylated substrates could persist for several days. To determine whether *Prmt1* is required for cell viability, we sought to derive a homozygous mutant ES cell line from preimplantation blastocysts. In our experience, ES cell lines are easier to derive from 129sv mice than from the C57BL/6 mice that harbor the *7.4.2* mutation. Therefore, the *Prmt1* mutation was crossed for 3 generations into 129sv mice. F_3 mice heterozygous for the provirus were interbred, and blastocysts were collected at E3.5 and cultured as described in Materials and Methods. Individual cell lines were established from 9 out of 40 blastocysts, of which 5 were homozygous for the *Prmt1* mutation. All mutant cell lines appeared morphologically similar to other ES cell lines and grew with doubling times similar to that of wild-type ES cells (approximately 12 h; data not shown).

***Prmt1* is not required for cell viability.** U3 gene trap vectors were designed to disrupt cellular gene expression by terminating transcription at one of two poly(A) sites (one in each LTR) carried by the provirus (14). Previous studies found high levels of a 4.7-kb βGeo transcript in 7.4.2 cells, approximately the size expected for *Prmt1*-βGeo fusion transcripts that terminate in the 5′ LTR. To test whether the *7.4.2* provirus disrupted expression of the *Prmt1* gene, homozygous mutant cell lines (Fig. 8A) were analyzed by Northern and Western blotting. Transcripts of 1.3 kb were detected in the wild-type and heterozygous cell lines, but not in the two mutant cell lines, using *Prmt1* cDNA sequences downstream of the site of provirus integration as a probe (Fig. 8B). Similarly, the Prmt1 protein was detected in extracts from wild-type and heterozygous cells but not in those from homozygous mutant cells (Fig. 8C). Levels of *Prmt1* transcripts in mutant cells were estimated by RT-PCR after mixing of different amounts of wild-type RNA with a constant amount of mutant RNA (Fig. 8D). The PCR signal obtained after mixing of mutant RNA with a 100-fold dilution of wild-type RNA was clearly greater than that obtained with mutant RNA alone, whereas the 250-fold dilution did not enhance the amplification of *Prmt1* sequences. This suggests that mutant cells express approximately 1% of the

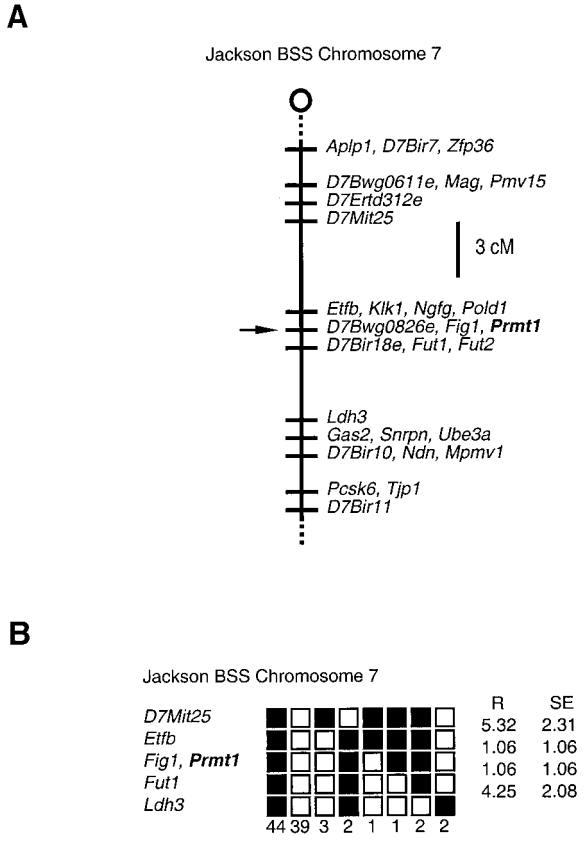

FIG. 7. *Prmt1* maps to the proximal end of chromosome 7. (A) Maps of Jackson Laboratory BSB and BSS backcrosses showing the proximal end of chromosome 7. The map is depicted with the centromere toward the top and a 3-centimorgan (cM) scale bar. Loci mapping to the same position are listed in alphabetical order. Missing typings were inferred from surrounding data where the assignment was unambiguous. Raw data from The Jackson Laboratory were obtained from the World Wide Web address http://www.jax.org/resources/documents/cmdata. (B) Haplotype of Jackson Laboratory BSB and BSS backcrosses showing the proximal end of chromosome 7 with loci linked to *Prmt1*. Loci are listed in order, with the most proximal at the top. The black boxes represent the C57BL6/JEi allele, and the white boxes represent the SPRET/Ei allele. The number of animals with each haplotype is at the bottom of each column of boxes. Percent recombination (R) between adjacent loci is given to the right, along with the standard error (SE) of each R value.

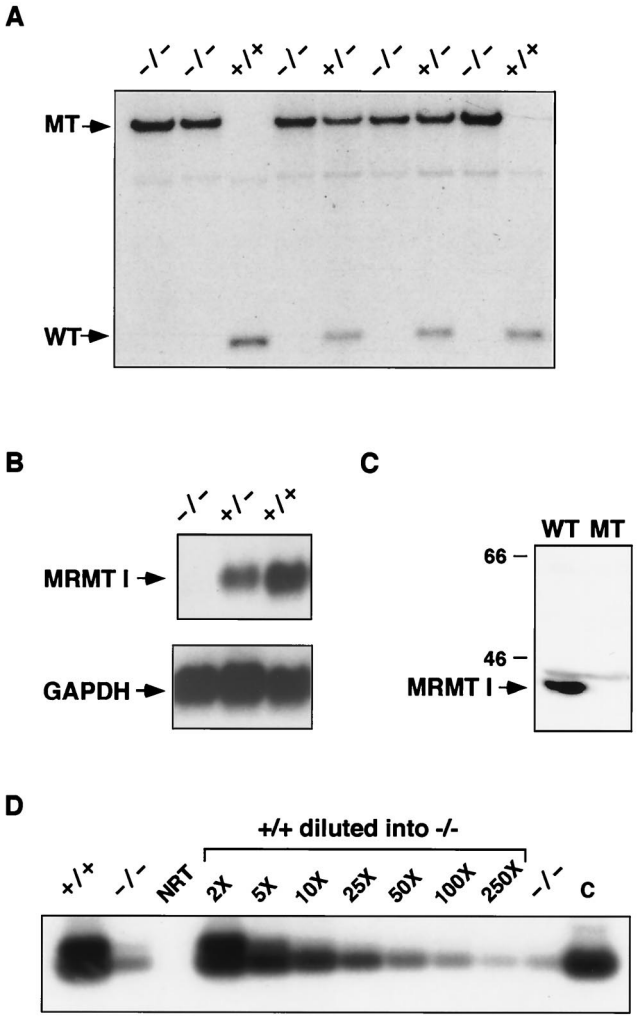

FIG. 8. Prmt1 is not required for cell viability. (A) ES cell lines were derived from E3.5 blastocysts and genotyped by Southern analysis. *Stu*I-digested DNA samples from wild-type (+/+), heterozygous (+/−), and homozygous mutant (−/−) ES cells was analyzed by hybridization to the 1.3-kb *Stu*I fragment containing the site of provirus integration. The genotype of each sample is shown along the top, and the mobility of the wild-type (WT) and mutant (MT) alleles is indicated on the left. (B) Selected cell lines were grown without feeder cells for 2 generations and analyzed by Northern blot hybridization. The murine *Prmt1* cDNA detects a single 1.35-kb transcript in the wild-type and heterozygous cell lines. Expression is ablated in mutant cells, indicating that Prmt1 is not essential for cell growth. A glyceraldehyde phosphate dehydrogenase (GAPDH) probe was used to ensure equal loading of RNA for each sample. (C) Western blot analysis of Prmt1 expression. A 200-μg protein sample from *Prmt1*$^{+/+}$ (WT) or *Prmt1*$^{-/-}$ (MT) cells was analyzed by Western blot analysis using an antibody against the rat PRMT1 protein. The values to the left are molecular sizes in kilodaltons. (D) RT-PCR analysis of *Prmt1* transcripts in wild-type and mutant ES cells. Cells were grown for 9 passages without feeder layers. Samples analyzed by RT-PCR contained 5 μg of RNA from wild-type (lane +/+) and mutant (left lane −/−) cells, 2.5 μg of RNA from mutant cells (right lane −/−), or 2.5 μg of RNA from mutant cells to which different dilutions of wild-type DNA had been added (lanes with the final dilution factors indicated). For example, lanes 2× and 5× contain 2.5 μg of mutant RNA mixed with 2.5 and 1 μg of wild-type RNA, respectively. Lane NRT shows an analysis of wild-type RNA minus reverse transcriptase. Lane C shows PCR products using 2 ng of *Prmt1* cDNA as a positive control. Levels of *Prmt1* transcripts in mutant cells appeared to be comparable to 1/100 of the wild-type levels.

wild-type level of *Prmt1* transcripts. We conclude that the *7.4.2* provirus severely disrupts Prmt1 expression and that the protein is not required for cell viability.

Loss of arginine methyltransferase activity in homozygous mutant ES cells. Although Prmt1 is orthologous to the predominant arginine methyltransferase expressed in mammalian cells, other enzymes are known to have type 1 activity (32). In addition, loss of Prmt1 could lead to a compensatory increase in the expression or activity of other methyltransferases. We therefore examined total methyltransferase activities in wild-type and Prmt1 mutant cells. As shown in Fig. 9A, *Prmt1*$^{-/-}$ cells expressed approximately eight times less methyltransferase activity than *Prmt1*$^{+/+}$cells, as assayed with an optimal synthetic-peptide substrate (21). This reduction is comparable to the contribution by Prmt1 orthologs to the total methyltransferase activity in other cell types, as estimated biochemically (12, 31). Therefore, we conclude that Prmt1 is the major type I enzyme in ES cells and that loss of Prmt1 activity does not result in a major compensatory increase in other methyltransferases.

Hypomethylation of cell proteins in *Prmt1*-deficient cells. Mutations in RMT, a type I enzyme of yeast, result in increased levels of hypomethylated substrates (12). Therefore, two types of experiments were performed to examine the methylation status of proteins in *Prmt1*$^{-/-}$ cells. First, total proteins extracted from *Prmt1*$^{-/-}$ and *Prmt1*$^{+/+}$ cells were tested for methyl acceptor activity when mixed with wild-type cell extracts. As shown in Fig. 9B, the methyl acceptor activity of total protein isolated from mutant cells was approximately 15 times greater than that observed for proteins from wild-type cells. The fact that proteins from wild-type cells proved to be such poor substrates suggests that most potential substrates are blocked by prior methylation, as has been observed with nucleolin and fibrillarin, which exist in a fully methylated state developmentally in vivo (18, 19). Second, the methylarginine content of cellular proteins was measured following acid hydrolysis and high-pressure liquid chromatography. As shown in Fig. 9C, total levels of asymmetric dimethylarginine were approximately twofold lower in Prmt1-deficient cells than in wild-type cells (54% ± 1.5% reduction based on three independent pairs of samples) whereas levels of monomethylarginine and symmetric dimethylarginine were slightly increased.

DISCUSSION

We previously described methods for using *lacZ*-based vectors to screen for mutations in regulated genes (25, 28). The present study characterized one of these mutant cell lines, termed 7.4.2, generated by an inserted U3βGeo provirus. The 7.4.2 cell line showed an increase in *lacZ* expression upon differentiation of ES cells into embryoid bodies (28). We show here that the gene disrupted by the provirus encodes the murine arginine methyltransferase 1 enzyme (EC 2.1.1.23). Embryos homozygous for the mutation arrest in development prior to E6.5, indicating that protein methylation is required for early postimplantation development. However, cell lines derived from homozygous mutant embryos are viable despite the fact that Prmt1 enzyme levels and the extent of protein methylation are significantly reduced.

cDNAs encoding Prmt1 were characterized as part of our analysis of the *7.4.2* mutation. As previously reported for the human gene, *Prmt1* transcripts are alternatively spliced to generate coding sequences for proteins of 353 or 371 amino acids. Overall, murine Prmt1 shares 100 and 95% sequence identity with the rat and human proteins, respectively. Phylogenetic conservation of the two proteins suggests that each has a distinct function, possibly related to substrate specificity or regulation of enzyme activity. Finally, *Prmt1* was mapped to mouse chromosome 7 in a region syntenic with the region of human chromosome 19q, where the human gene had been previously mapped (29). Neither region is associated with disease loci in mice or humans.

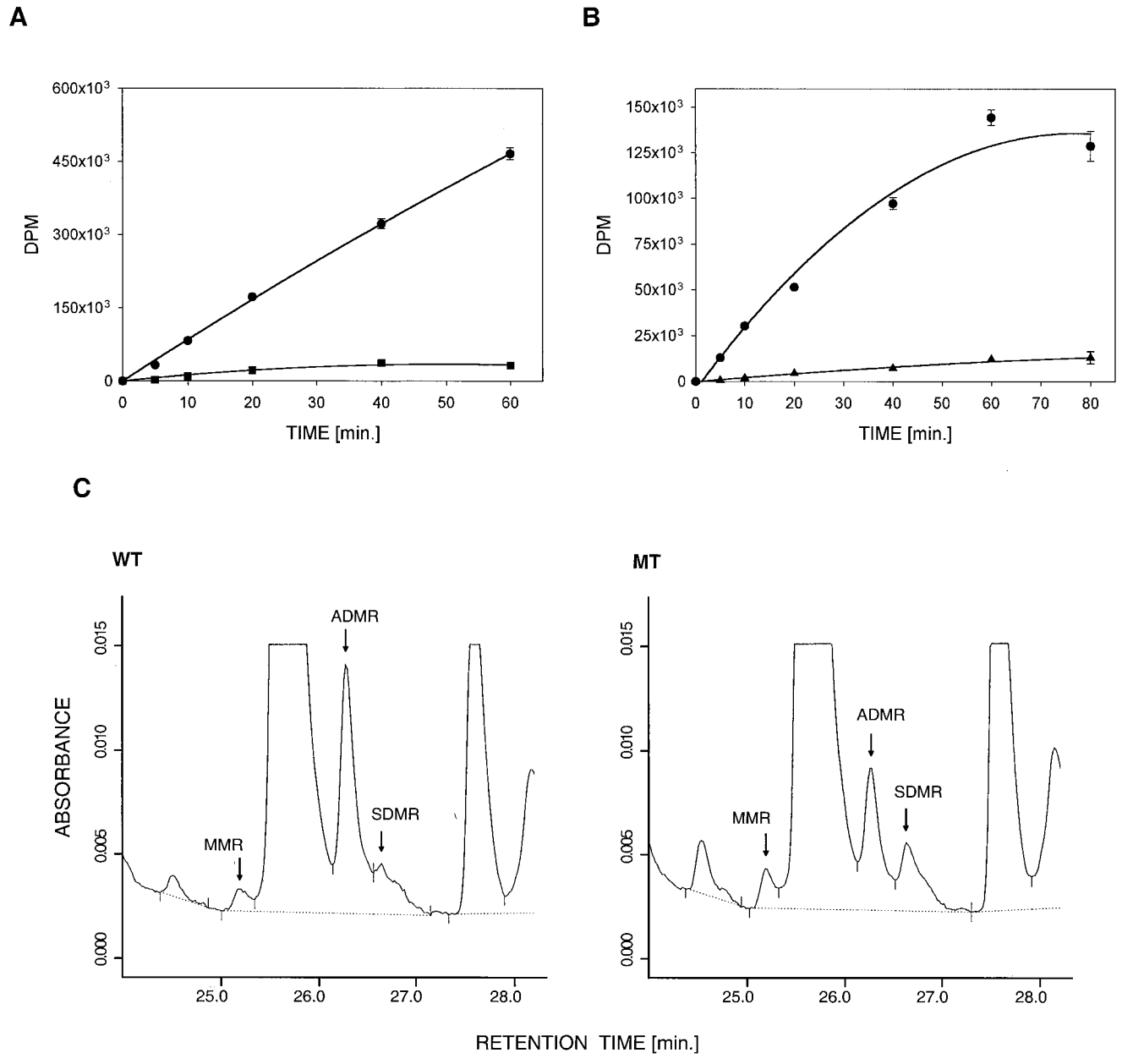

FIG. 9. Reduced Prmt1 activity in *Prmt1*$^{-/-}$ cells increases the steady-state levels of hypomethylated substrates. (A) Arginine *N*-methyltransferase activities in wild-type and *Prmt1* mutant cells. Extracts (20 μg of protein) from *Prmt1*$^{+/+}$ (circles) and *Prmt1*$^{-/-}$ (squares) cells were assayed for arginine *N*-methyltransferase activity using a synthetic RGG peptide as a substrate (100 μM). Levels of ^{3}H-methylated substrate were monitored by a filter binding assay. DPM, disintegrations per minute. (B) Hypomethylation of cellular proteins in *Prmt1*$^{-/-}$ cells. Extracts (20 μg of protein) from wild-type cells were mixed with an equal amount of protein from either *Prmt1*$^{-/-}$ (circles) or *Prmt1*$^{+/+}$ (triangles) cells, and the transfer of *methyl*-^{3}H groups from *S*-adenosyl-L-[*methyl*-^{3}H]methionine into cellular proteins was monitored by a filter binding assay. (C) Analysis of N^{G}-monomethylarginine (MMR), asymmetric N^{G},N^{G}-dimethylarginine (ADMR), and symmetric N^{G},N'^{G}-dimethylarginine (SDMR) in wild-type (WT) and Prmt1-deficient mutant (MT) cells. Total cellular protein (20 μg) from *Prmt1*$^{+/+}$ and *Prmt1*$^{-/-}$ cells was subjected to acid hydrolysis and analyzed by high-pressure liquid chromatography.

Our analysis of *Prmt1* expression confirms earlier reports describing widespread expression of the orthologous rat and human genes in all of the tissues examined (17, 29, 32). In addition, all of the tissues examined expressed both spliced forms of the murine gene. Expression of the inserted β-galactosidase marker was highest in developing neural structures. This is potentially significant in light of previous studies showing high levels of methyltransferase activity in the developing brain that decline after birth (22). However, homozygous mutant embryos die close to the time when the *Prmt1* gene is first induced, as assessed by β-galactosidase staining, and well before the onset of neural development. As early embryonic death appears to be a common consequence of mutations disrupting basic cellular processes (7), the phenotype is consistent with the important role Prmt1 is thought to play in RNA metabolism. For example, the timing of embryonic death is similar to that observed with a mutation in *Fug1*, which encodes the RAN GTPase-activating protein (8), and is earlier than that observed with a mutation in hnRNP C, a highly abundant, ubiquitous constituent of nuclear riboprotein com-

plexes (35). Both RAN GAP and hnRNP C appear to function in RNA biogenesis and transport.

By comparing the levels of enzyme activity in extracts from wild-type and *Prmt1*-deficient cells, we showed that Prmt1 accounts for over 85% of the total arginine methyltransferase activity in ES cells, as assayed using an optimal (21) synthetic RGG substrate. However, Prmt1 is responsible for just over 50% of the normal steady-state levels of N^G,N^G-dimethylarginine present in cellular proteins. Therefore, other arginine methyltransferases, presumably with different substrate specificities, appear to make significant contributions to the total dimethylarginine content of the cell. Such enzymes could include PRMT3 and HRMT1L1, type I-related enzymes that modify RGG substrates poorly, if at all (29, 32).

The methylation status of cellular proteins was also assessed by testing their capacity to be methylated in vitro. Prmt1, present in wild-type cell extracts, was incubated with proteins isolated from either wild-type or Prmt1-deficient cells in the presence of *S*-adenosyl-L-*methyl*-[^{3}H]methionine. While proteins from wild-type cells had negligible acceptor activity, proteins from Prmt1-deficient cells were significantly hypomethylated. This has two implications. First, the function of Prmt1 appears to be nonredundant, since other cellular enzymes compensate for no more than a small part of the lost Prmt1 activity. Second, as previously observed with nucleolin and fibrillarin (18, 19), most potential substrates in normal cells appear to be blocked by prior methylation. Our analysis does not exclude the possibility that individual substrates are present in a hypomethylated state in ES cells or that the methylation status may change in response to different physiological conditions. Hypomethylated proteins may also exist only transiently, for example, during a specific step in a biochemical process. However, this latter possibility would require an arginine demethylase, an activity that has not yet been identified in mammalian cells. Experiments to study potential dynamic changes in protein methylation are in progress.

In summary, this report describes the first mutation in a mammalian arginine methyltransferase. These enzymes have been implicated in a wide variety of cellular processes, including cell proliferation, signal transduction, and protein trafficking. The availability of Prmt1-deficient cells will assist efforts to identify physiological substrates and to understand the function of the enzyme in normal cellular metabolism.

ACKNOWLEDGMENTS

We thank Harvey Herschman for the gift of anti-Prmt1 antibody, Abudi Nashabi for technical assistance, Eric Howard for measurements of protein methylarginine content, and Lucy Rowe, Mary Barter, and Lois Maltais of The Jackson Laboratory for assistance with gene mapping and nomenclature.

This work was supported by Public Health Service grants (R01HG00684, R01GM51201, and R01RR13166 to H.E.R.) and by a grant from the Kleberg Foundation. Additional support was provided by an NCI Cancer Center Support Grant (P30CA42014) to the Vanderbilt-Ingram Cancer Center. M.J.R. was supported by a Medical Scientist Training Grant (5T32-GM07347).

REFERENCES

1. **Abramovich, C., B. Yakobson, J. Chebath, and M. Revel.** 1997. A protein-ginine methyltransferase binds to the intracytoplasmic domain of the IFNAR1 chain in the type I interferon receptor. EMBO J. **16:**260–266.
2. **Altschul, S. F., T. L. Madden, A. A. Schaffer, J. Zhang, Z. Zhang, W. Miller, and D. J. Lipman.** 1997. Gapped BLAST and PSI-BLAST: a new generation of protein database search programs. Nucleic Acids Res. **25:**3389–3402.
3. **Byvoet, P., G. R. Shepherd, J. M. Hardin, and B. J. Noland.** 1972. The distribution and turnover of labeled methyl groups in histone fractions of cultured mammalian cells. Arch. Biochem. Biophys. **148:**558–567.
4. **Chen, D., H. Ma, H. Hong, S. S. Koh, S. M. Huang, B. T. Schurter, D. W. Aswad, and M. R. Stallcup.** 1999. Regulation of transcription by a protein methyltransferase. Science **284:**2174–2177.
5. **Chomczynski, P., and N. Sacchi.** 1987. Single-step method of RNA isolation by acid guanidinium thiocyanate-phenol-chloroform extraction. Anal. Biochem. **162:**156–159.
6. **Cimato, T. R., M. J. Ettinger, X. Zhou, and J. M. Aletta.** 1997. Nerve growth factor-specific regulation of protein methylation during neuronal differentiation of PC12 cells. J. Cell Biol. **138:**1089–1103.
7. **Copp, A. J.** 1995. Death before birth: clues from gene knockouts and mutations. Trends Genet. **11:**87–93.
8. **DeGregori, J., A. Russ, H. von Melchner, H. Rayburn, P. Priyaranjan, N. A. Jenkins, N. G. Copeland, and H. E. Ruley.** 1994. A murine homolog of the yeast RNA1 gene is required for postimplantation development. Genes Dev. **8:**265–276.
9. **Fahrner, K., B. L. Hogan, and R. A. Flavell.** 1987. Transcription of H-2 and Qa genes in embryonic and adult mice. EMBO J. **6:**1265–1271.
10. **Feinberg, A. P., and B. Vogelstein.** 1984. A technique for radiolabelling DNA restriction endonuclease fragments to high specific activity. Anal. Biochem. **137:**266–267.
11. **Gary, J. D., and S. Clarke.** 1998. Protein arginine methyltransferases. Prog. Nucleic Acid Res. **61:**65–133.
12. **Gary, J. D., W. J. Lin, M. C. Yang, H. R. Herschman, and S. Clarke.** 1996. The predominant protein-arginine methyltransferase from Saccharomyces cerevisiae. J. Biol. Chem. **271:**12585–12594.
13. **Henry, M. F., and P. A. Silver.** 1996. A novel methyltransferase (Hmt1p) modifies poly(A)$^+$-RNA-binding proteins. Mol. Cell. Biol. **16:**3668–3678.
14. **Hicks, G. G., E.-G. Shi, J. Chen, M. Roshon, D. Williamson, C. Scherer, and H. E. Ruley.** 1995. Retrovirus gene traps. Methods Enzymol. **254:**263–275.
15. **Kawasaki, E. S.** 1990. Amplification of RNA, p. 21–27. *In* M. A. Innis, D. H. Gelfand, J. J. Sninsky, and T. J. White (ed.), PCR protocols: a guide to methods and applications. Academic Press, San Diego, Calif.
16. **Kim, B. R., and K. H. Yang.** 1991. Effects of sinefungin and 5′-deoxy-5′-S-isobutyl-adenosine on lipopolysaccharide-induced proliferation and protein N-methylation of arginyl residues in murine splenic lymphocytes. Toxicol. Lett. **59:**109–116.
17. **Lin, W. J., J. D. Gary, M. C. Yang, S. Clarke, and H. R. Herschman.** 1996. The mammalian immediate-early TIS21 protein and the leukemia-associated BTG1 protein interact with a protein-arginine N-methyltransferase. J. Biol. Chem. **271:**15034–15044.
18. **Lischwe, M. A., R. G. Cook, Y. S. Ahn, L. C. Yeoman, and H. Busch.** 1985. Clustering of glycine and NG,NG-dimethylarginine in nucleolar protein C23. Biochemistry **24:**6025–6028.
19. **Lischwe, M. A., R. L. Ochs, R. Reddy, R. G. Cook, L. C. Yeoman, E. M. Tan, M. Reichlin, and H. Busch.** 1985. Purification and partial characterization of a nucleolar scleroderma antigen (Mr = 34,000; pI, 8.5) rich in NG,NG-dimethylarginine. J. Biol. Chem. **260:**14304–14310.
20. **Liu, Q., and G. Dreyfuss.** 1995. In vivo and in vitro arginine methylation of RNA-binding proteins. Mol. Cell. Biol. **15:**2800–2808.
21. **Najbauer, J., B. A. Johnson, A. L. Young, and D. W. Aswad.** 1993. Peptides with sequences similar to glycine, arginine-rich motifs in proteins interacting with RNA are efficiently recognized by methyltransferase(s) modifying arginine in numerous proteins. J. Biol. Chem. **268:**10501–10509.
22. **Paik, W. K., S. Kim, and H. W. Lee.** 1972. Protein methylation during the development of rat brain. Biochem. Biophys. Res. Commun. **46:**933–941.
23. **Pintucci, G., N. Quarto, and D. B. Rifkin.** 1996. Methylation of high molecular weight fibroblast growth factor-2 determines post-translational increases in molecular weight and affects its intracellular distribution. Mol. Biol. Cell **7:**1249–1258.
24. **Rajpurohit, R., W. K. Paik, and S. Kim.** 1994. Effect of enzymic methylation of heterogeneous ribonucleoprotein particle A1 on its nucleic-acid binding and controlled proteolysis. Biochem. J. **304:**903–909.
25. **Reddy, S., H. Rayburn, H. von Melchner, and H. E. Ruley.** 1992. Fluorescence-activated sorting of totipotent embryonic stem cells expressing developmentally regulated lacZ fusion genes. Proc. Natl. Acad. Sci. USA **89:**6721–6725.
26. **Rowe, L. B., J. H. Nadeau, R. Turner, W. N. Frankel, V. A. Letts, J. T. Eppig, M. S. Ko, S. J. Thurston, and E. H. Birkenmeier.** 1994. Maps from two interspecific backcross DNA panels available as a community genetic mapping resource. Mamm. Genome **5:**253–274.
27. **Sambrook, J., E. F. Fritsch, and T. Maniatis.** 1989. Molecular cloning: a laboratory manual, 2nd ed. Cold Spring Harbor Laboratory Press, Cold Spring Harbor, N.Y.
28. **Scherer, C. A., J. Chen, A. Nachabeh, N. Hopkins, and H. E. Ruley.** 1996. Transcriptional specificity of the pluripotent embryonic stem cell. Cell Growth Differ. **7:**1393–1401.
29. **Scott, H. S., S. E. Antonarakis, M. D. Lalioti, C. Rossier, P. A. Silver, and M. F. Henry.** 1998. Identification and characterization of two putative human arginine methyltransferases (HRMT1L1 and HRMT1L2). Genomics **48:**330–340.
30. **Shen, E. C., M. F. Henry, V. H. Weiss, S. R. Valentini, P. A. Silver, and M. S. Lee.** 1998. Arginine methylation facilitates the nuclear export of hnRNP proteins. Genes Dev. **12:**679–691.
31. **Tang, J., A. Frankel, R. J. Cook, S. Kim, W. K. Paik, K. R. Williams, S.**

Clarke, and H. R. Herschman. 2000. PRMT1 is the predominant type I protein arginine methyltransferase in mammalian cells. J. Biol. Chem. **275:** 7723–7730.
32. **Tang, J., J. D. Gary, S. Clarke, and H. R. Herschman.** 1998. PRMT 3, a type I protein arginine N-methyltransferase that differs from PRMT1 in its oligomerization, subcellular localization, substrate specificity, and regulation. J. Biol. Chem. **273:**16935–16945.
33. **Valentini, S. R., V. H. Weiss, and P. A. Silver.** 1999. Arginine methylation and binding of Hrp1p to the efficiency element for mRNA 3′-end formation. RNA **5:**272–280.
34. **Vanet, A., J. A. Plumbridge, and J. H. Alix.** 1993. Cotranscription of two genes necessary for ribosomal protein L11 methylation (*prmA*) and pantothenate transport (*panF*) in *Escherichia coli* K-12. J. Bacteriol. **175:**7178–7188.
35. **Williamson, D. J., J. DeGregori, S. Banik-Maiti, and H. E. Ruley.** 2000. hnRNP C is required for postimplantation mouse development but is dispensable for cell viability. Mol. Cell. Biol. **20:**4094–4105.